

# Additive manufacturing of porous lattices with spatially optimized permeability

David B. Robinson, Declan T. Mahaffey-Dowd, Carly Hui, Bernice E. Mills, Maher Salloum, Denis Ridzal, Drew P. Kouri, John Miers

## Flow in Lattices

Many chemical engineering technologies rely on intimate contact between a moving fluid and a porous solid. New additive manufacturing (AM) technologies create opportunities to precisely control the architecture of a porous solid,<sup>1,2</sup> and push the performance envelopes of these technologies. To take full advantage of these opportunities, we seek AM techniques that create small pores within large parts. We are using computational simulation and optimization methods to design porous solids,<sup>3,4</sup> printing prototype structures with a commercial partner, and verifying print accuracy using x-ray tomography.

## Design of High-Resolution, Diagonally Oriented Cube-Edge Lattices

For high fluid-solid contact, we desire micrometer-scale pores that only photopolymer 3D printers can achieve. Images are projected into a resin, adding a layer of solid cubes at each illuminated pixel. We propose unit cells requiring only a few printed cubes. The cube-edge unit cell shown allows for flow in 3 dimensions. A column aligned with the cube body diagonal enables lateral mixing. The unit cell must be aligned with the printed cubes, so the column is aligned with the cube diagonals.

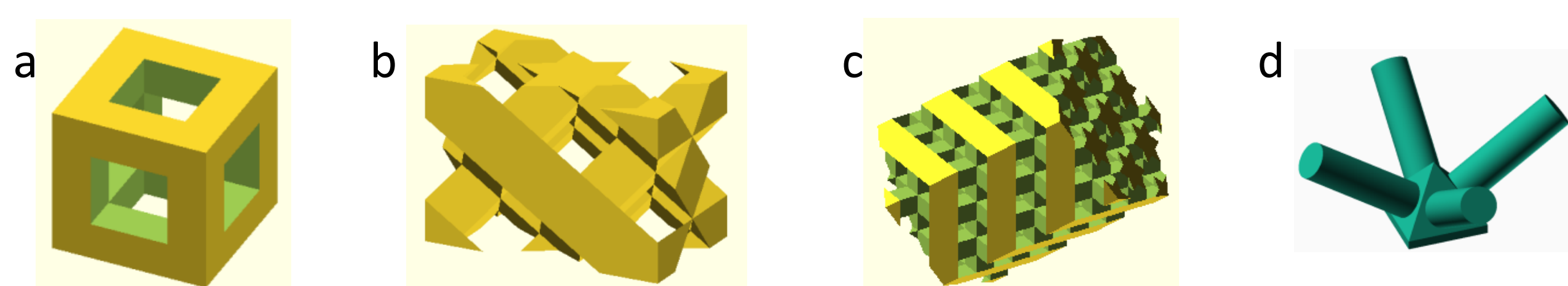


Fig. 1. (a) Cube-edge unit cell. (b) Rectangular prism unit cell composed of cube-edge unit cells with body diagonals aligned vertically. (c) Column derived from the unit cell in (b). (d) A part with 4 columns.

## Evaluation of Manufactured Photopolymer Lattices

ty (pore volume fraction) 0.5. Cubic cells are parallel to the

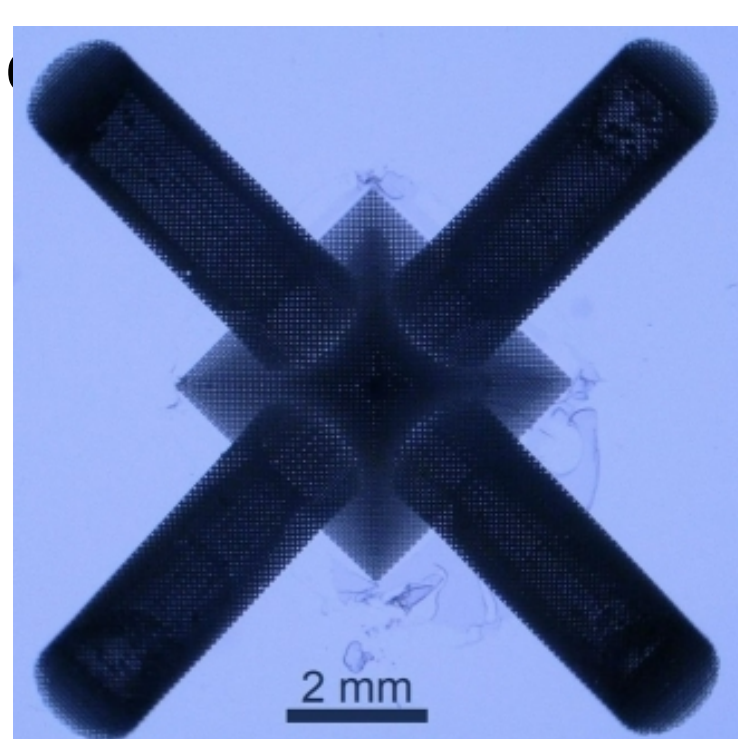


Fig. 2. Optical micrograph of part printed by Acrea3D.

X-ray tomography combines x-ray transmission images collected at many angles to create a 3D grayscale representation. We chose a threshold to identify solid vs. void and digitally aligned the parts for comparison. The thresholding process can make it difficult to accurately determine porosity, but we can use the results to identify how well the shape and size of the unit cells matches the designed parts, and whether sparse point, line, or plane defects are present.

Slices of the designed part are a uniform array of sharp triangular features. The built part shows more rounded features, unit cells that are not perfectly aligned, and sparse defects. One defect is circled.

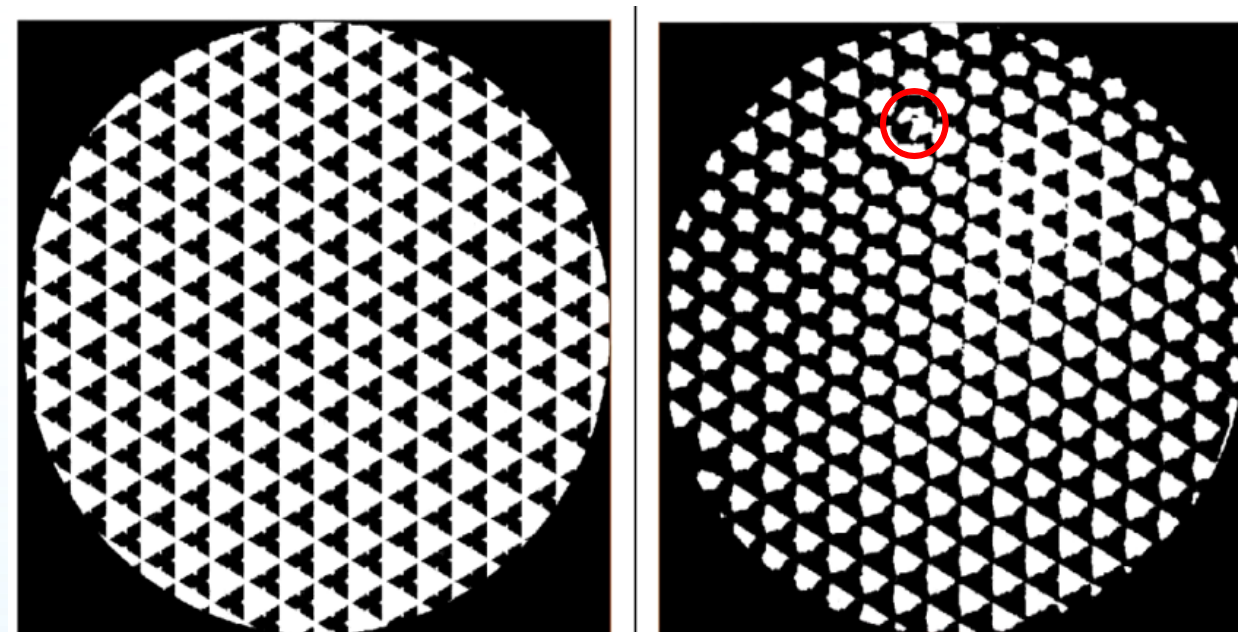


Fig. 3. Slices of the part perpendicular to a cylinder axis. Left: as designed. Right: as printed, and measured by x-ray tomography. White is solid and black is void.

## Computed Flow Properties

Slow flow through porous materials can be modeled by Darcy's Law, relating a macroscopic velocity  $v$  to the pressure gradient, fluid viscosity  $\mu$ , and permeability  $\kappa$ . We desire a relationship between  $\kappa$ , the unit cell size  $D$ , and porosity  $\varepsilon$ .

$$\text{Darcy's Law: } v = \frac{\kappa}{\mu} \nabla p$$

Using COMSOL numerical modeling software, we have computed the  $\kappa(D, \varepsilon)$  relationships for a cube-edge lattice by solving the Navier-Stokes equations for a column of 4x4x10 rectangular unit cells. The data can be fit as:  $\kappa = \frac{D^2 \varepsilon^2}{8\pi} (0.056 + 0.42\varepsilon)$ . The lattice permeability is lower than that of a square array of cylindrical tubes with the same  $D$  and  $\varepsilon$ , presumably due to narrower channels, sharp corners and zigzag flow paths.

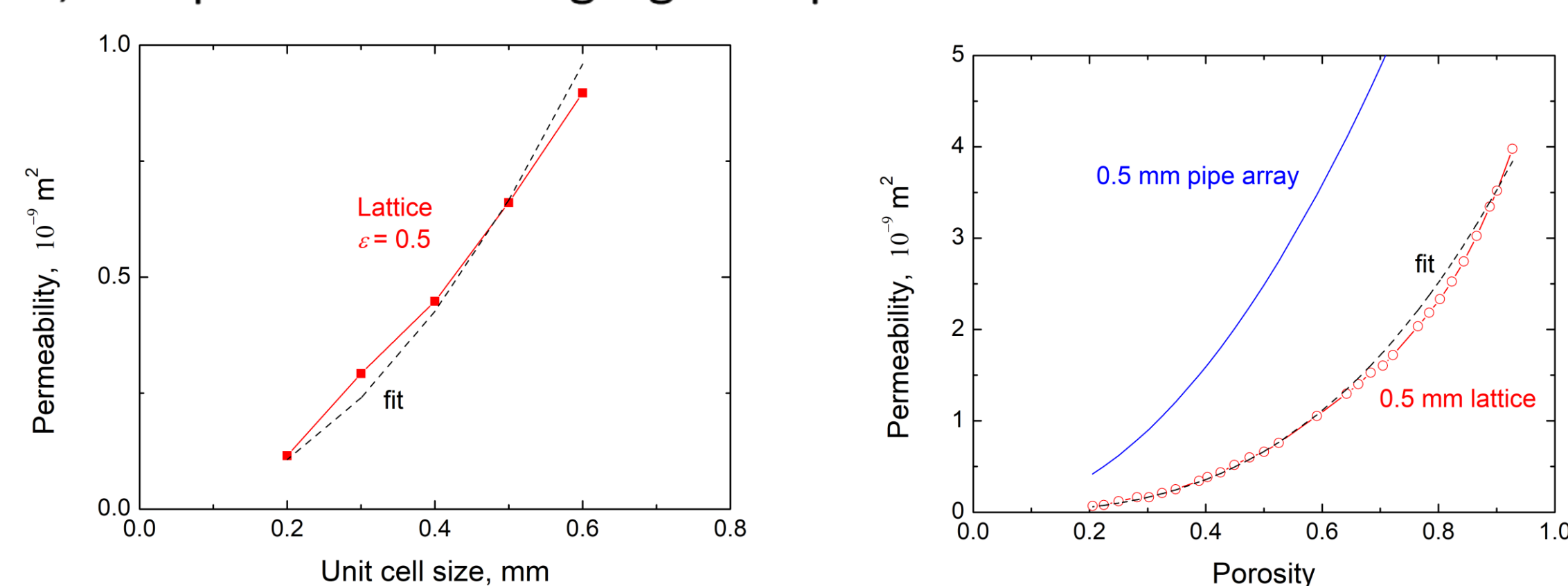
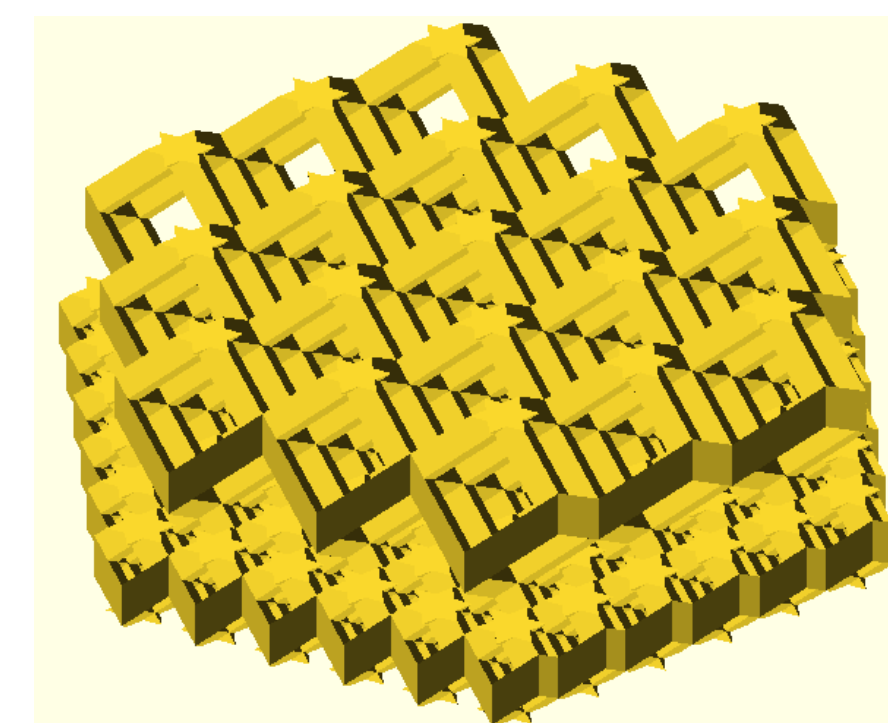


Fig. 4. Calculated permeability as a function of (left) unit cell size and (right) porosity.

Using this relationship, we can adjust  $D$ , and porosity  $\varepsilon$  by changing unit cell or strut size by appropriate factors, and achieve precise local adjustment of the fluid flow.

Fig. 5. Illustration of large unit cells tiled on a layer of smaller unit cells.

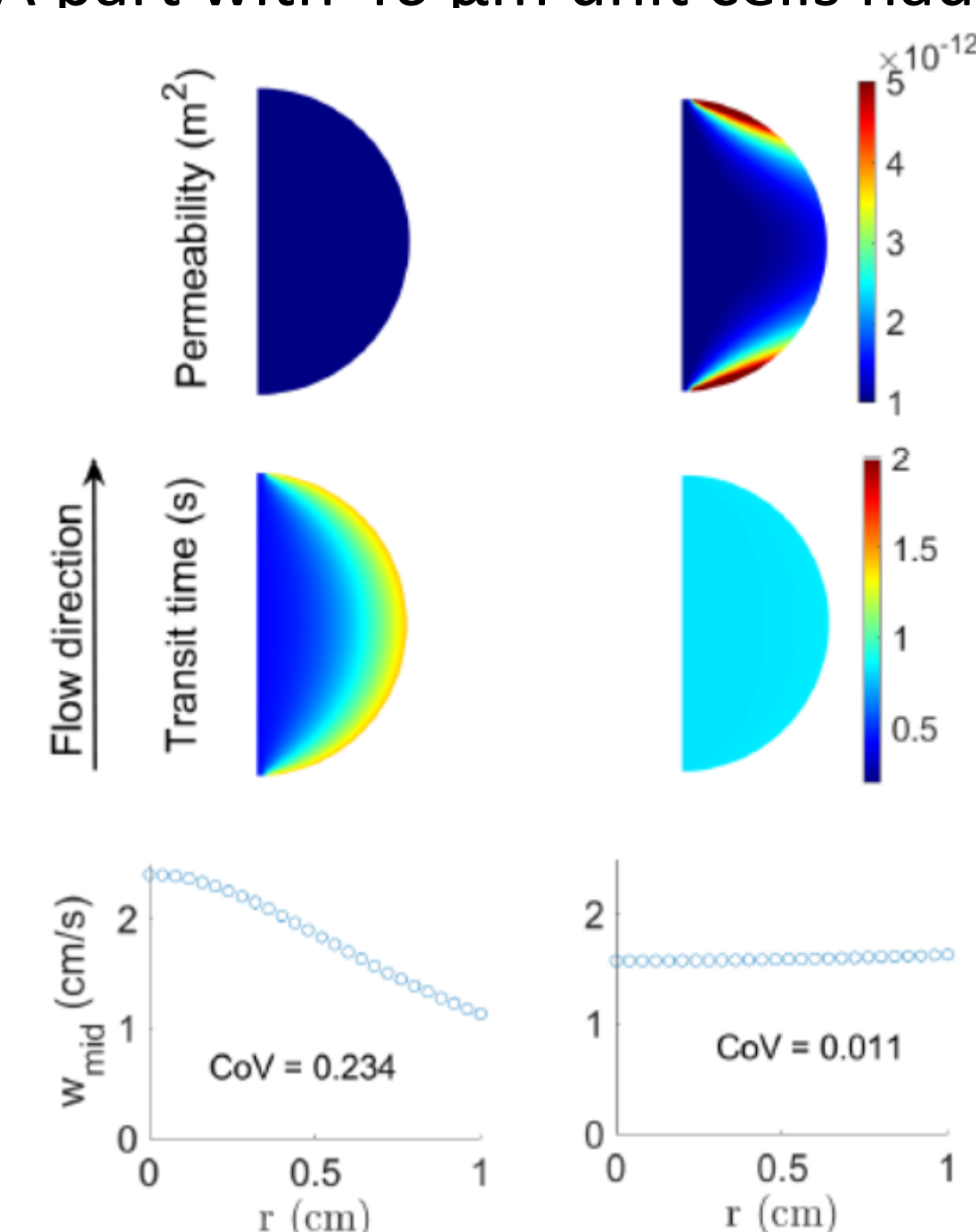


## Optimized Flow Properties

If we model a column that is spherical instead of cylindrical, with a uniform permeability, the midplane velocity and transit times are nonuniform.

Optimization algorithms show that if the permeability is higher near the inlet and outlet, this can be corrected. Our lattices should enable testing of this prediction.

Fig. 6. Permeability, transit time, and midplane velocity for (left) uniform and (right) optimized permeability in a spherical column.



## Conclusions

Additive manufacturing techniques enable novel architectures for porous media. Our lattices approximately follow  $\kappa \propto D^2 \varepsilon^2$  and likely allow more precise tuning of permeability than porous media made from randomly packed powders. We predict that optimized grading of permeability can achieve desired fluid velocity fields and transit times in flow columns. We aspire to apply these methods to practical applications in the handling of renewable fuels such as hydrogen, and electrochemical energy devices.

## References

1. I. R. Woodward et al. Scalable 3D-printed lattices for pressure control in fluid applications. *AIChE J.* 67:e17452, 2021.
2. M. Klumpp et al. Periodic open cellular structures with ideal cubic cell geometry: Effect of porosity and cell orientation on pressure drop behavior. *Chem. Eng. J.* 242 (2014) 364–378.
3. M. Salloum and D.B. Robinson. A Numerical model of exchange chromatography through 3-D lattice structures, *AIChE J.* 64(5), 1874-1884, 2018
4. D.B. Robinson. 3D-Printed Apparatus for Efficient Fluid-Solid Contact. US Patent 10493693 B1 (2019).